Circulating tumor cell detection using photoacoustic spectral methods

Eric M. Strohm, Elizabeth S. L. Berndl, Michael C. Kolios*
Department of Physics, Ryerson University, Toronto, Canada;
*mkolios@ryerson.ca

ABSTRACT

A method to detect and differentiate circulating melanoma tumor cells (CTCs) from blood cells using ultrasound and photoacoustic signals with frequencies over 100 MHz is presented. At these frequencies, the acoustic wavelength is similar to the dimensions of a cell, which results in unique features in the signal; periodically varying minima and maxima occur throughout the power spectrum. The spacing between minima depends on the ratio of the size to sound speed of the cell. Using a 532 nm pulsed laser and a 375 MHz center frequency wide-bandwidth transducer, the ultrasound and photoacoustic signals were measured from single cells. A total of 80 cells were measured, 20 melanoma cells, 20 white blood cells (WBCs) and 40 red blood cells (RBCs). The photoacoustic spectral spacing Δf between minima was 95 ± 15 MHz for melanoma cells and greater than 230 MHz for RBCs. No photoacoustic signal was detected from WBCs. The ultrasonic spectral spacing between minima was 46 ± 9 MHz for melanoma cells and 98 ± 11 for WBCs. Both photoacoustic and ultrasound signals were detected from melanoma cells, while only ultrasound signals were detected from WBCs. RBCs showed distinct photoacoustic spectral variations in comparison to any other type of cell. Using the spectral spacing and signal amplitudes, each cell type could be grouped together to aid in cell identification. This method could be used for label-free counting and classifying cells in a sample.

Keywords: Photoacoustics, circulating tumor cells, high frequency ultrasound, spectral analysis

1. INTRODUCTION

Cancer cells that circulate in the blood stream are known as circulating tumor cells (CTCs). These are tumor cells that are shed from a primary tumor and can metastasize elsewhere in the body, resulting in a secondary tumor. CTCs are common in patients with cancer, but not in healthy people[1]. Tumors can shed cells at early stages of growth prior to detection of the primary tumor[2–4], with lower blood concentrations of CTCs related to a favourable outcome[5–10]. Detection of CTCs in blood could potentially be used as a clinical screening tool and prognosis estimator.

Several methods have been developed to detect CTCs from blood samples, including flow cytometry[11,12], immunomagnetic bead enrichment[13,14] and photoacoustic detection [15–19]. In photoacoustic methods, a laser irradiates the sample. Cells that absorb the laser energy emit a photoacoustic wave that can be detected using an ultrasound transducer. Optical absorption of energy by the cell is required to generate a photoacoustic signal; this can be endogenous absorbing components such as hemoglobin (in red blood cells) or melanin (in melanocytes). Photoacoustic studies have exploited the optically absorbing properties of melanoma cells to detect these cells circulating in the bloodstream. Alternatively, dyes or nanoparticles can be added that selectively bind to specific cells to facilitate photoacoustic wave generation[20–27].

All other photoacoustic studies have used transducers with frequencies less than 60 MHz, which are primarily used for image generation. At these frequencies, the photoacoustic signal spectrum is generally flat and featureless. For cells in the 5-30 μm range, the photoacoustic and ultrasound signal spectra have unique features in the 100-500 MHz range that are directly related to the size and sound speed of the cell[28]. Periodically varying minima and maxima occur throughout the power spectrum where the spacing between minima depends directly on the ratio of the cell diameter to sound speed. As the cell diameter increases, the location and spacing between frequency minima decreases, and as the sound speed increases, the frequency minima and spacing between spectral features increases. These spectral features cannot be detected with traditional photoacoustic methods using frequencies under 100 MHz. Blood contains cells such as red blood cells (RBCs) and a variety of white blood cells (WBCs) which have distinct variations in size, shape and composition. The only cells that absorb visible light are RBCs, as melanoma cells should not be present. This proof of concept study uses the spectral spacing and signal amplitude to aid in identifying and differentiating cells in a sample, particularly circulating melanoma cells.

Photons Plus Ultrasound: Imaging and Sensing 2014, edited by Alexander A. Oraevsky, Lihong V. Wang,
Proc. of SPIE Vol. 8943, 89430D · © 2014 SPIE · CCC code: 1605-7422/14/$18 · doi: 10.1117/12.2040124

2. METHOD

2.1 Cell Preparation

Blood was extracted from a healthy male volunteer in accordance with the Ryerson Ethics Board (REB #2012-210). Using a lancet, a drop of blood was extracted from the fingertip and deposited into one mL of Dulbecco's modified eagle medium (DMEM). The diluted blood was transferred to a glass bottom dish (Mattek, USA) with a thin layer of 1% agar lining the bottom. The WBCs and RBCs could be differentiated by optical observation, however, the WBC sub-type could not be identified. Murine melanoma (B16-F1) cells were cultured with DMEM containing 10% fetal bovine serum (FBS) and kept at 37°C with 5% CO_2. When confluent, the cells were dissociated using trypsin and added to a fresh glass bottom dish containing 1% agar. The agar is required to prevent the cells from adhering to the dish, and also prevents back reflections during acoustic measurements.

2.2 Photoacoustic Microscope

A SASAM photoacoustic microscope (Kibero GmbH, Germany) was used for all measurements. In this system, a transducer was positioned above the sample holder of an IX81 inverted optical microscope (Olympus, Japan). The transducer and microscope optics were co-aligned, enabling simultaneous optical and acoustic measurements. A 532 nm laser (Teem Photonics, France) was focused through a side port of the microscope and onto the sample holder using a 10x optical objective to an approximately 5 µm diameter spot size. A dish containing cells to be examined was placed in the microscope, and the transducer aligned to the focal spot of the optical lens. The stage was moved to target specific cells in the sample while maintaining alignment between the transducer and optics. The photoacoustic microscope and measurement schematic are shown in Figure 1. Pulse echo ultrasound measurements were made using a transducer with a center frequency of 375 MHz and a monocycle pulse generator with a pulse repetition rate of 4 kHz. Laser pulses were generated at a pulse repetition rate of 4 kHz (alternating with the ultrasound pulses) and both the ultrasound echo and the photoacoustic signal generated from the cell were digitized in a single a-line at 8 GS/s. The laser energy ranged from 40 to 250 nJ per pulse. All signals were amplified by a 40 dB amplifier (Miteq, USA) and averaged 100 times to increase the signal to noise ratio (SNR). The signals were normalized by removing the transducer response, then a Hamming window applied and the spectrum calculated using the Fast Fourier transform. Further details on the instrument can be found in reference[29], and details on the signal processing methods including normalization can be found in reference[30].

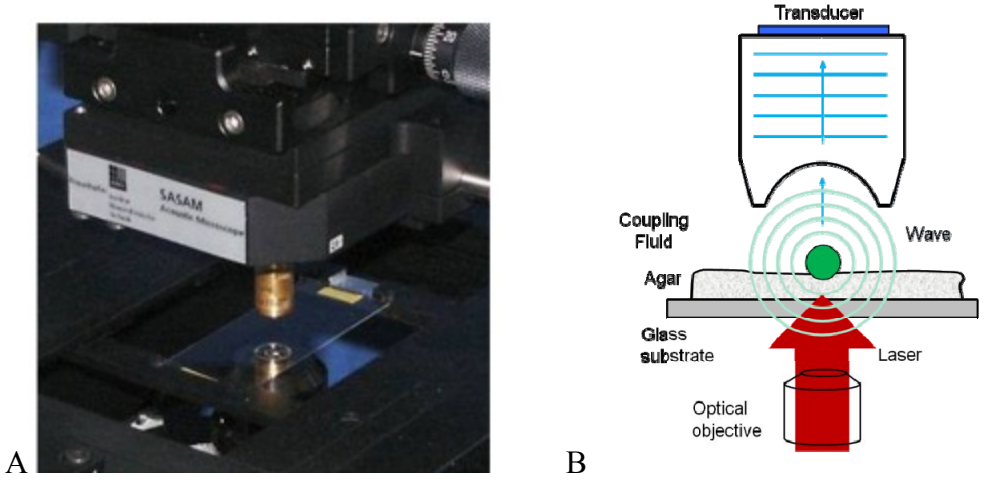

Figure 1: The photoacoustic microscope. (A) The sample holder, showing the optics and the transducer positioned above the sample. (B) A schematic showing the operation of the photoacoustic microscope. During photoacoustic measurements, the transducer passively records the signals. In ultrasound mode, ultrasound pulses travel down through the transducer and focused through a sapphire lens, and then the transducer records the resulting echoes from the sample. Image of the acoustic microscope courtesy of Kibero GmbH.

3. RESULTS AND DISCUSSION

The photoacoustic and ultrasound signals from 80 cells were measured: 40 RBCs, 20 WBCs and 20 melanoma cells. The goal was to differentiate these cells using the signal amplitude, spectral features and whether an ultrasound and/or photoacoustic signal was recorded. Simultaneous optical imaging along with photoacoustic and ultrasound measurements of a single cell were recorded; this enabled positive identification of the cell type after a measurement. Figure 2 shows an optical image of the cells measured and how the cell types can be identified prior to measurement. The RBCs and WBCs were measured from freshly extracted human blood, while the melanoma cells were cultured and measured separately. While the cells could be identified and differentiated according to optical observation, the goal of this study was to compare the ultrasound and photoacoustic features of known cells so that cells in a sample containing unknown cells could be identified.

The photoacoustic and ultrasound time domain signal measured from the different cells are shown in figures 3 and 4, respectively. The photoacoustic spectrum of the RBC is known to vary depending on its orientation[31], therefore the photoacoustic signal is shown from a single RBC in the two extreme orientations, horizontal and vertical. It is difficult to differentiate the cell types from the time domain signal alone; the spectrum of these cells is shown in Figure 5. In these spectra, periodically varying minima and maxima occur at different frequencies, where the spectral spacing between minima (Δf) is related to the size and sound speed of the cell. The average ultrasound spectral spacing for the melanoma and WBCs was 46±9 MHz and 98±11 MHz, respectively, while the average photoacoustic spectral spacing for the melanoma and RBCs was 95±15 MHz and ranging between 230-400 MHz, respectively. Some RBCs were measured in a horizontal orientation (see figure 3A) and thus the spectrum was flat; these RBCs were assigned a Δf 400 MHz. Melanoma cells are larger than either WBCs or WBCs, and thus the spectral spacing is smaller. RBCs have a higher sound speed than the other cells (~1700 m/s vs. approximately 1560 m/s for both melanoma and WBCs), and also have a unique shape where the spectrum depends the orientation of the cell; thus the spectral spacing Δf is significantly larger than the other cells. Table 1 summarizes the results of the measurements.

The ultrasound and photoacoustic signal amplitude was used as another metric to help differentiate the cell types. In photoacoustic measurements, the recorded photoacoustic signal is directly related to the absorption coefficient of cell, the laser intensity used, as well as the size and sound speed within the cell[28]. The photoacoustic peak-peak signal amplitude was recorded for each cell. A different laser energy was used to measure the RBCs and melanoma cells, therefore the signal amplitude was normalized to the laser energy for direct comparison. The photoacoustic signal amplitude was 60±36 and 23±13 mV_{pp}/nJ for melanoma cells and RBCs, respectively. No photoacoustic signal was measured from WBCs; this is expected, as the absorption properties of WBCs at 532 nm is negligible. In ultrasound, the ultrasound echo signal amplitude is related to the incident wave amplitude, as well as the physical properties of the cell[32]. The same incident pulse was used for all measurements and therefore normalization across different cells was not required. The ultrasound signal amplitude was 17±6 and10±2 mV_{pp} for WBCs and melanoma cells, respectively. These results are summarized in table 1.

The average ultrasound and photoacoustic signal amplitude and spectral spacing Δf is different for each cell type. This can be visualized by plotting the signal amplitude vs. spectral spacing for each cell as shown in Figure 6. For the ultrasound measurements, the melanoma cells and WBCs can be grouped separately, while for the photoacoustic measurements, the melanoma cells have a distinct grouping compared to the RBCs. The accuracy of cell identification can be improved by considering whether an ultrasound signal and/or photoacoustic signal is recorded. Only ultrasound signals would be recorded from WBCs as they have negligible absorption at 532 nm. Both ultrasound and photoacoustic signals are recorded from melanoma cells. Both signals are recorded from RBCs as well, however it is unlikely any cell would have a spectral spacing comparable to RBCs, which is over 200 MHz.

A small number of cells were measured for this proof of principle study (80 total), in which the cells measured were already known. Cell types could be differentiated using the ultrasound and photoacoustic signal amplitude and spectral spacing Δf. These measurements could be used to count and identify the different cell types in a sample, including identifying circulating melanoma tumor cells without the use of external additives such as dyes. For use in a clinic, the method would require high speed counting which is not practical using the microscope. These techniques could be translated to a flow device with comparable function as flow cytometry.

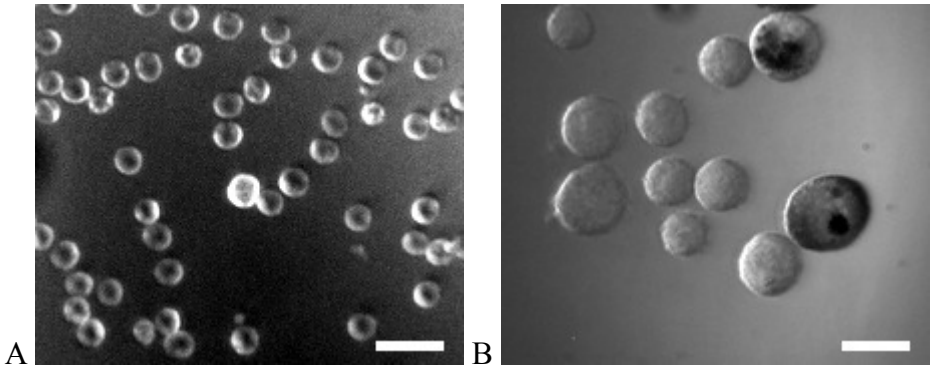

Figure 2: Optical images of (A) RBCs and a WBC (middle of image), and (B) melanoma cells during a measurement in the acoustic microscope. The scale bar is 20 μm. Noise is present due to low light conditions.

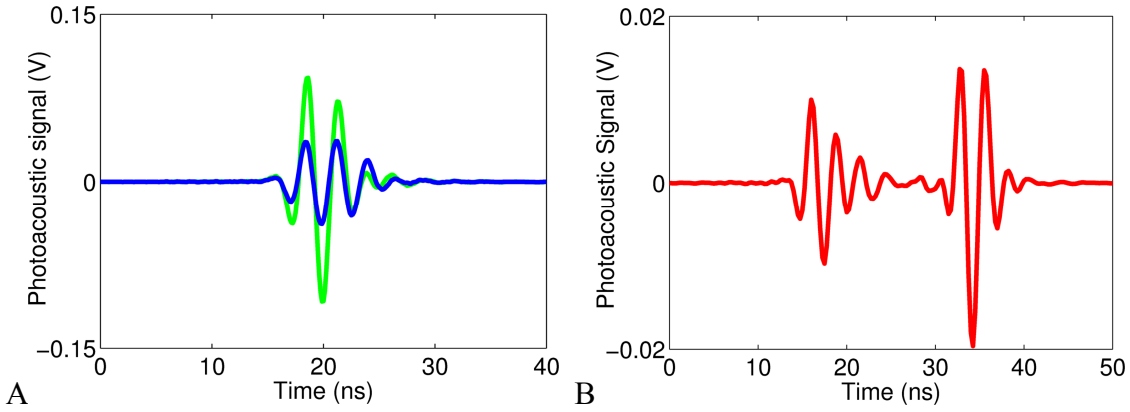

Figure 3: Typical time domain photoacoustic signals recorded directly from (A) a RBC in a horizontal (green) and vertical (blue) orientation, and (B) a melanoma cell (red).

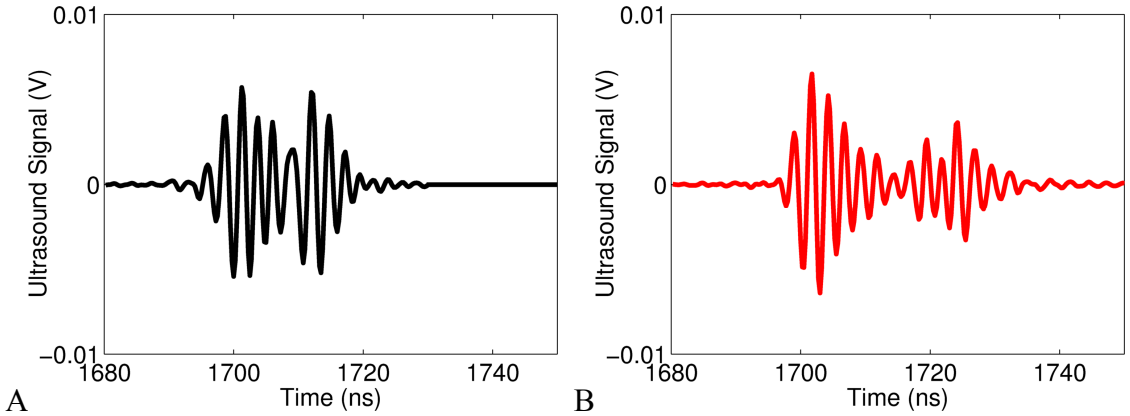

Figure 4: Typical time domain ultrasound signals recorded directly from (A) a WBC (black) and (B) a melanoma cell (red). A Hamming window was applied between 1680-1730 ns in (A), and 1680-1750 ns in (B) to remove artifacts that occur during the measurement.

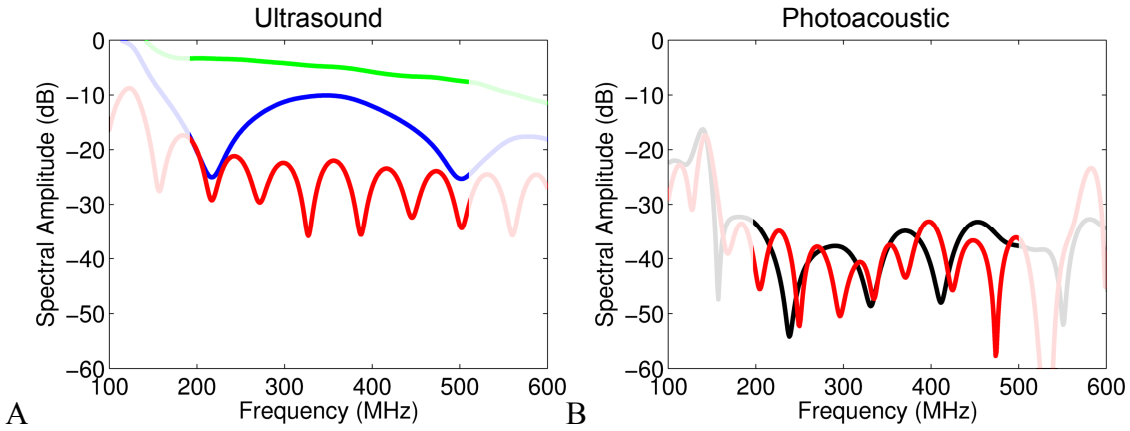

Figure 5: Typical photoacoustic and ultrasound power spectra from cells. (A) Photoacoustic spectra from a melanoma (red) and a RBC in two orientations, horizontal (green) and vertical (blue). (B) Ultrasound spectra from a melanoma cell (red) and a WBC (black). The area outside of the transducer bandwidth is noise and has been grayed.

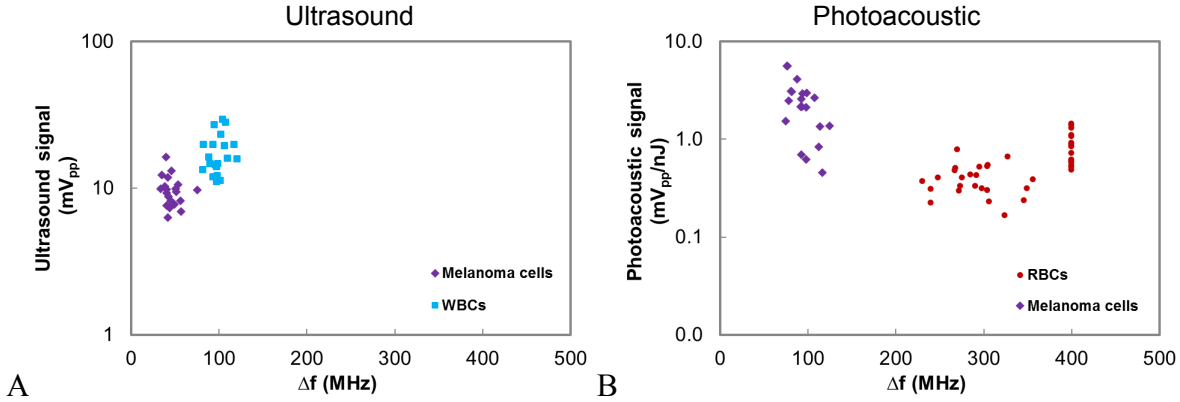

Figure 6: The measured ultrasound peak-peak signal (A) and normalized photoacoustic signal (B) of cells vs. their spectral spacing Δf. The position of cells in this graph can be used to identify them. Only an ultrasound signal is recorded from WBCs, while both a photoacoustic and ultrasound signal is recorded from melanoma cells. RBCs also have both an ultrasound and photoacoustic signal, however, the photoacoustic spectral spacing Δf is much larger than the others and the ultrasound signal is not used. RBC spectra that were flat and contained no spectral minima were assigned a Δf value of 400 MHz, thus creating the vertical column in the figure.

Cell	Number measured	Ultrasound Spectral Spacing (MHz)	Ultrasound Signal Amplitude (mV_{pp})	Photoacoustic Spectral Spacing (MHz)	Photoacoustic Signal Amplitude (mV_{pp}/nJ)
WBC	20	98 ± 11	17± 6	-	-
Melanoma	20	46 ± 9	10 ± 2	95 ± 15	60 ± 36
RBC	40	-	-	230-400	23 ± 13

Table 1: A summary of the ultrasound and photoacoustic spectral spacing and signal amplitude for the different cell types. A total of 80 cells were measured: 20 melanoma cells, 20 WBCs and 40 RBCs.

4. CONCLUSIONS

This proof of concept study has demonstrated that high frequency ultrasound and photoacoustic methods using the signal amplitude and spectral features can be used to differentiate types of cells that can be found in blood. WBCs and RBCs can be identified according to these parameters. In particular, Melanoma circulating tumor cells could be detected from their unique signals using label-free methods.

5. ACKNOWLEDGEMENTS

This research was undertaken, in part, thanks to funding from the Natural Sciences and Engineering Research Council of Canada, the Canadian Cancer Society and the Canada Research Chairs Program awarded to M. Kolios. Funding to purchase the equipment was provided by the Canada Foundation for Innovation, the Ontario Ministry of Research and Innovation, and Ryerson University. This study was supported, in part, by the Ontario Institute for Cancer Research Network through funding provided by the Province of Ontario.

REFERENCES

[1] Allard, W.J., Matera, J., Miller, M.C., Repollet, M., Connelly, M.C., Rao, C., Tibbe, A.G.J., Uhr, J.W., and Terstappen, L.W.M.M., "Tumor Cells Circulate in the Peripheral Blood of All Major Carcinomas but not in Healthy Subjects or Patients With Nonmalignant Diseases," Clinical Cancer Research 10(20), 6897–6904 (2004).

[2] Butler, T.P., and Gullino, P.M., "Quantitation of Cell Shedding into Efferent Blood of Mammary Adenocarcinoma," Cancer Research 35(3), 512–516 (1975).

[3] Liotta, L.A., Kleinerman, J., and Saidel, G.M., "Quantitative Relationships of Intravascular Tumor Cells, Tumor Vessels, and Pulmonary Metastases following Tumor Implantation," Cancer Research 34(5), 997–1004 (1974).

[4] Chambers, A.F., Groom, A.C., and MacDonald, I.C., "Metastasis: Dissemination and growth of cancer cells in metastatic sites," Nature Reviews Cancer 2(8), 563–572 (2002).

[5] Cristofanilli, M., Budd, G.T., Ellis, M.J., Stopeck, A., Matera, J., Miller, M.C., Reuben, J.M., Doyle, G.V., Allard, W.J., et al., "Circulating Tumor Cells, Disease Progression, and Survival in Metastatic Breast Cancer," New England Journal of Medicine 351(8), 781–791 (2004).

[6] Riethdorf, S., and Pantel, K., "Advancing personalized cancer therapy by detection and characterization of circulating carcinoma cells," Annals of the New York Academy of Sciences 1210(1), 66–77 (2010).

[7] Hayes, D.F., Cristofanilli, M., Budd, G.T., Ellis, M.J., Stopeck, A., Miller, M.C., Matera, J., Allard, W.J., Doyle, G.V., et al., "Circulating Tumor Cells at Each Follow-up Time Point during Therapy of Metastatic Breast Cancer Patients Predict Progression-Free and Overall Survival," Clinical Cancer Research 12(14), 4218–4224 (2006).

[8] Riethdorf, S., Fritsche, H., Müller, V., Rau, T., Schindlbeck, C., Rack, B., Janni, W., Coith, C., Beck, K., et al., "Detection of Circulating Tumor Cells in Peripheral Blood of Patients with Metastatic Breast Cancer: A Validation Study of the CellSearch System," Clinical Cancer Research 13(3), 920–928 (2007).

[9] Cohen, S.J., Punt, C.J.A., Iannotti, N., Saidman, B.H., Sabbath, K.D., Gabrail, N.Y., Picus, J., Morse, M., Mitchell, E., et al., "Relationship of Circulating Tumor Cells to Tumor Response, Progression-Free Survival, and Overall Survival in Patients With Metastatic Colorectal Cancer," Journal of Clinical Oncology 26(19), 3213–3221 (2008).

[10] Budd, G.T., Cristofanilli, M., Ellis, M.J., Stopeck, A., Borden, E., Miller, M.C., Matera, J., Repollet, M., Doyle, G.V., et al., "Circulating Tumor Cells versus Imaging—Predicting Overall Survival in Metastatic Breast Cancer," Clinical Cancer Research 12(21), 6403–6409 (2006).

[11] Terstappen, L., Rao, C., Gross, S., Kotelnikov, V., Racilla, E., Uhr, J., and Weiss, A., "Flowcytometry - Principles and Feasibility in Transfusion Medicine. Enumeration of Epithelial Derived Tumor Cells in Peripheral Blood," Vox Sanguinis 74(S2), 269–274 (1998).

[12] Simpson, S.J., Vachula, M., Kennedy, M.J., Kaizer, H., Coon, J.S., Ghalie, R., Williams, S., and Van Epps, D., "Detection of tumor cells in the bone marrow, peripheral blood, and apheresis products of breast cancer patients using flow cytometry," Experimental Hematology 23(10), 1062 (1995).

[13] Zieglschmid, V., Hollmann, C., and Böcher, O., "Detection of disseminated tumor cells in peripheral blood," Critical Reviews in Clinical Laboratory Sciences 42(2), 155–196 (2005).

[14] Hardingham, J.E., Kotasek, D., Farmer, B., Butler, R.N., Mi, J.-X., Sage, R.E., and Dobrovic, A., "Immunobead-PCR: A Technique for the Detection of Circulating Tumor Cells Using Immunomagnetic Beads and the Polymerase Chain Reaction," Cancer Research 53(15), 3455–3458 (1993).

[15] Weight, R.M., Viator, J. a, Dale, P.S., Caldwell, C.W., and Lisle, A.E., "Photoacoustic detection of metastatic melanoma cells in the human circulatory system," Optics Letters 31(20), 2998–3000 (2006).
[16] Galanzha, E.I., Shashkov, E.V., Spring, P.M., Suen, J.Y., and Zharov, V.P., "In vivo, Noninvasive, Label-Free Detection and Eradication of Circulating Metastatic Melanoma Cells Using Two-Color Photoacoustic Flow Cytometry with a Diode Laser," Cancer Research 69(20), 7926–7934 (2009).
[17] Gutierrez-Juarez, G., Gupta, S.K., Al-Shaer, M., Polo-Parada, L., Dale, P.S., Papageorgio, C., and Viator, J. a, "Detection of melanoma cells in vitro using an optical detector of photoacoustic waves," Lasers in Surgery and Medicine 42(3), 274–81 (2010).
[18] Nedosekin, D.A., Sarimollaoglu, M., Ye, J., Galanzha, E.I., and Zharov, V.P., "In vivo ultra fast photoacoustic flow cytometry of circulating human melanoma cells using near infrared high pulse rate lasers," Cytometry Part A 79A(10), 825–833 (2011).
[19] O'Brien, C.M., Rood, K., Sengupta, S., Gupta, S.K., DeSouza, T., Cook, A., and Viator, J.A., "Detection and Isolation of Circulating Melanoma Cells using Photoacoustic Flowmetry," Journal of Visualized Experiments (57), (2011).
[20] Viator, J.A., Gupta, S., Goldschmidt, B.S., Bhattacharyya, K., Kannan, R., Shukla, R., Dale, P.S., Boote, E., and Katti, K., "Gold Nanoparticle Mediated Detection of Prostate Cancer Cells Using Photoacoustic Flowmetry with Optical Reflectance," Journal of Biomedical Nanotechnology 6(2), 187–191 (2010).
[21] McCormack, D.R., Bhattacharyya, K., Kannan, R., Katti, K., and Viator, J. A., "Enhanced photoacoustic detection of melanoma cells using gold nanoparticles," Lasers in Surgery and Medicine 43(4), 333–8 (2011).
[22] Zharov, V.P., Galanzha, E.I., Shashkov, E.V., Kim, J.-W., Khlebtsov, N.G., and Tuchin, V.V., "Photoacoustic flow cytometry: principle and application for real-time detection of circulating single nanoparticles, pathogens, and contrast dyes in vivo," Journal of Biomedical Optics 12(5), 051503–051503–14 (2007).
[23] Galanzha, E.I., Shashkov, E.V., Kelly, T., Kim, J.-W., Yang, L., and Zharov, V.P., "In vivo magnetic enrichment and multiplex photoacoustic detection of circulating tumour cells," Nature Nanotechnology 4(12), 855–860 (2009).
[24] Hu, X., Wei, C.-W., Xia, J., Pelivanov, I., O'Donnell, M., and Gao, X., "Trapping and Photoacoustic Detection of CTCs at the Single Cell per Milliliter Level with Magneto-Optical Coupled Nanoparticles," Small 9(12), 2046–2052 (2013).
[25] Wei, C.-W., Xia, J., Pelivanov, I., Hu, X., Gao, X., and O'Donnell, M., "Trapping and dynamic manipulation of polystyrene beads mimicking circulating tumor cells using targeted magnetic/photoacoustic contrast agents," Journal of Biomedical Optics 17(10), 101517–1 (2012).
[26] Galanzha, E.I., Shashkov, E., Sarimollaoglu, M., Beenken, K.E., Basnakian, A.G., Shirtliff, M.E., Kim, J.-W., Smeltzer, M.S., and Zharov, V.P., "In Vivo Magnetic Enrichment, Photoacoustic Diagnosis, and Photothermal Purging of Infected Blood Using Multifunctional Gold and Magnetic Nanoparticles," PLoS ONE 7(9), e45557 (2012).
[27] Qian, X., Peng, X.-H., Ansari, D.O., Yin-Goen, Q., Chen, G.Z., Shin, D.M., Yang, L., Young, A.N., Wang, M.D., et al., "In vivo tumor targeting and spectroscopic detection with surface-enhanced Raman nanoparticle tags," Nature Biotechnology 26(1), 83–90 (2008).
[28] Diebold, G.J., Khan, M.I., and Park, S.M., "Photoacoustic 'Signatures' of Particulate Matter: Optical Production of Acoustic Monopole Radiation," Science 250(4977), 101–104 (1990).
[29] Strohm, E.M., Czarnota, G.J., and Kolios, M.C., "Quantitative measurements of apoptotic cell properties using acoustic microscopy," IEEE Transactions on Ultrasonics, Ferroelectrics and Frequency Control 57(10), 2293–2304 (2010).
[30] Strohm, E.M., Gorelikov, I., Matsuura, N., and Kolios, M.C., "Acoustic and photoacoustic characterization of micron-sized perfluorocarbon emulsions," Journal of Biomedical Optics 17(9), 096016–1–9 (2012).
[31] Strohm, E.M., Elizabeth S.L. Berndl, and Kolios, M.C., "Probing red blood cell morphology using high frequency photoacoustics," Biophysical Journal 105(1), 59–67 (2013).
[32] Anderson, V.C., "Sound Scattering from a Fluid Sphere," The Journal of the Acoustical Society of America 22(4), 426 (1950).